



POLİTEKNİK DERGİSİ

JOURNAL of POLYTECHNIC

ISSN: 1302-0900 (PRINT), ISSN: 2147-9429 (ONLINE)



Analytical solution of a multi-winding coil problem with an air core in spherical coordinates

Hava çekirdekli çok sargılı bobbin probleminin küresel koordinatlarda analitik çözümü

Yazar(lar) (Author(s)): Hüseyin YILDIZ¹, Erol UZAL², Hüseyin ÇALIK³

ORCID¹: 0000-0002-0575-3904

ORCID²: 0000-0003-0008-1376

ORCID³: 0000-0001-8298-8945

To cite to this article): Yıldız H., Uzal E. ve Çalık H., “Analytical solution of a multi-winding coil problem with an air core in spherical coordinates”, *Journal of Polytechnic*, 27(1): 255-261, 2024).

Bu makaleye şu şekilde atıfta bulunabilirsiniz:Yıldız H., Uzal E. ve Çalık H., “Analytical solution of a multi-winding coil problem with an air core in spherical coordinates”, *Politeknik Dergisi*, 27(1): 255-261, 2024).

Erişim linki (To link to this article): <http://dergipark.org.tr/politeknik/archive>

DOI: 10.2339/politeknik.1052918

Analytical Solution of a Multi-Winding Coil Problem With an Air Core in Spherical Coordinates

Highlights

- ❖ An analytical calculations for multi-winding coils around a air core in spherical coordinates.
- ❖ The magnetic field distribution and compare with FEA results (2D).
- ❖ Analytical calculation of self-inductance coefficient in spherical coordinate .
- ❖ Analytical calculation of mutual inductance coefficients in spherical coordinate.
- ❖ The variation of mutual inductance coefficient with γ was investigated.

Graphical Abstract

In this study, the A and B expressions of a multi-winding air-core coil were calculated analytically. Compared with FEA results. The variation of the mutual inductance coefficient with γ was investigated by setting up the experimental setup.

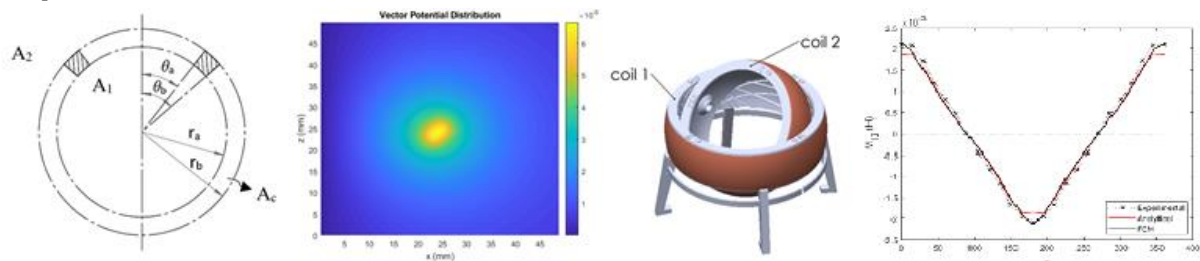


Figure. Problem descriptions and results

Aim

The aim of this study is to obtain analytical formulas that can be used for the solution of multi-winding coil problems in the spherical coordinates.

Design & Methodology

Maxwell's equations were solved in spherical coordinates. Parameters were determined to compare FEA and experimental results. FEA results were obtained using package programs. The experimental setup was set up and mutual inductance coefficients were obtained.

Originality

In this study, for the first time in the literature, analytical results have been obtained for the multi-winding coil problem in spherical coordinates. The accuracy of the obtained results has been demonstrated by comparing with FEA and experimental results.

Findings

Analytical formulas of A and B vectors were obtained for the multi-winding coil problem. The distribution of A and B on the plane was calculated by creating the FEA model. Analytical results and FEA results were found to be compatible. By setting up the experimental setup, the variation of the mutual inductance coefficient depending on γ was examined. Numerical data were obtained from the analytical results and compared with the experimental results.

Conclusion

It was seen that the results obtained at the end of the study were compatible with the FEA results and the experimental results. It has been seen that the results are very useful in the preliminary design of electromechanical systems with spherical geometry.

Declaration of Ethical Standards

The authors of this article declare that the materials and methods used in this study do not require ethical committee permission and/or legal-special permission.

Analytical Solution of a Multi-Winding Coil Problem With an Air Core in Spherical Coordinates

Araştırma Makalesi / Research Article

Hüseyin YILDIZ^{1*}, Erol UZAL², Hüseyin ÇALIK³

¹Department of Mechanical and Metal Technologies, Istanbul University – Cerrahpasa, Buyukcekmece, 34500, Istanbul, Turkey.

²Department of Mechanical Engineering, Istanbul University – Cerrahpasa, Avcilar, 34320, Istanbul, Turkey.

³Department of Electrical and Electronics Engineering, Giresun University, 28000, Giresun, Turkey.

(Geliş/Received : 03.01.2022 ; Kabul/Accepted : 07.06.2022 ; Erken Görünüm/Early View : 26.07.2022)

ABSTRACT

In this study, electromagnetic fields and mutual inductance of two interacting coils were computed analytically, and the results were compared with numerical solutions and measurements. For the analytical solution, the fields were expressed in spherical coordinates in each coil's frame. The total field due to two coils was calculated using superposition, resulting in infinite series involving associated Legendre functions. The numerical computations were carried out by finite element analysis capabilities of ANSYS Maxwell. At the end, the self-inductances and the mutual inductance coefficients between the coils (which depend on the angle between the coils) were computed. The results (analytical, finite element method, and the measurements) were compared, obtaining good agreement for various relative positions of the coils.

Keywords: Magnetic field; Maxwell's equations; mutual inductance; spherical coordinates.

Hava Çekirdekli Çok Sargılı Bobbin Porbleminin Küresel Koordinatlarda Analitik Çözümü

ÖZ

Bu çalışmada, bir biri ile etkileşen iki bobinin elektromanyetik alanı ve karşılıklı endüktans katsayısı analitik olarak hesaplanmış, sonuçlar sayısal çözümler ve ölçümlerle karşılaştırılmıştır. Analitik çözüm her bir bobinin etkisi küresel koordinatlarda genişletilerek hesaplandı. Her iki bobinden kaynaklanan toplam alanlar, süperpozisyon ilkesi gereği uyarlanmış legendre fonksiyonlarını içeren seri çözümler olarak elde edildi. Sayısal hesaplamalar ANSYS Maxwell programında sonlu elemanlar metodu kullanılarak elde edildi. Bobinlerin öz endüktans ve karşılıklı endüktans katsayıları (bobinler arasındaki açığa bağlı olarak) elde edildi. Sonuç olarak, elde edilen sonuçlar (analitik, sonlu elemanlar yöntemi ve ölçümler) kayaslanarak, bobinlerin çeşitli görelî konumları için analitik formüllerin geçerli oldukları gösterildi.

Anahtar Kelimeler: Manyetik alan, karşılıklı endüktans, küresel koordinatlar.

1. INTRODUCTION

Calculation of self and mutual inductances have central importance in many areas of science and technology, including traditional and novel electromechanical devices and brain simulation systems. General development of solution methods are summarized in the literature[1-2]. The vast majority of the studies have circular geometry. There are several studies about calculations for various combinations of circular loops, disc coils, solenoids and thick cylindrical coils. Solutions have also been developed for inductance calculations of non-coaxial coils[2-3]. There are studies investigating the analytical form of mutual inductance coefficient for coaxial thin and thick coils [4]. Analytical calculations of self-inductance (L) and mutual inductance coefficients (M_{ij}) in the spherical coordinate system has been receiving attention due to new technological structures with spherical geometry such as spherical 3 degrees-of-freedom electric actuators and brain stimulation systems.

Lipiriski et al. (1975) analytically calculated the magnetic and electric fields created by a spherical structure with axial symmetry[5]. Semenov analyzed the magnetic field and carried out inductance calculations for a coil in a linear and homogeneous isotropic environment with a magnetic permeability of empty space in an isolated magnetic field [6]. Eaton has developed an analytical method in spherical coordinates to quickly calculate the total electric field created by coils located in different regions in brain stimulation applications [7]. Matute (2005) obtained the analytical solution of Maxwell's equations with axial symmetry in the spherical coordinate system[8]. Liu et al. (2020) studied the sequential arrangement of a large number of coils in spherical coordinates to obtain a homogeneous magnetic field analytically[9]. Most of the studies include calculations of vector field potential \mathbf{A} , magnetic field \mathbf{B} , electric field \mathbf{E} and L and M_{ij} for a single-turn coil. In literature, analytical formulas for multi-winding coil structures are not yet available. So, FEM (Finite Element Method) is used to calculate \mathbf{E} , \mathbf{B} and torque (τ) magnitudes in the applications of electrical machines

*Sorumlu Yazar (Corresponding Author)
e-posta : huseyin.yildiz@iuc.edu.tr

with spherical geometry. For spherical induction motor studies the most important examples are [10 -16]. Although the analyses made in cartesian and cylindrical coordinates are sufficient for the design of traditional machines, they are still among the interesting topics today. However, in the analysis of structures with spherical geometry such as spherical electric motors and brain stimulation systems, solutions need to be obtained in spherical coordinates. So, the results obtained in the spherical coordinate system provide more precise and faster solutions due to them being analytical solutions[14][15][17].

2. GENERAL SEPARATED SOLUTION IN SPHERICAL COORDINATES

The differential form of Maxwell's equations in air (or free-space) are, in the SI system of units (bold-face letters are vectors) [18].

$$\nabla \cdot \mathbf{E} = \frac{1}{\epsilon_0} \rho \quad (1)$$

$$\nabla \cdot \mathbf{B} = 0 \quad (2)$$

$$\nabla \times \mathbf{E} = -\frac{\partial \mathbf{B}}{\partial t} \quad (3)$$

$$\nabla \times \mathbf{B} = \mu_0 \mathbf{J} + \mu_0 \epsilon_0 \frac{\partial \mathbf{E}}{\partial t} \quad (4)$$

Here μ_0 and ϵ_0 are the magnetic permeability and dielectric permittivity of free space (or air, very approximately). ρ and \mathbf{J} are free electric charge density and current density. In our case, free charges are zero, and the current density is only due to the applied currents on the coils and will be given as time-harmonic functions. Electric and magnetic fields (\mathbf{E} and \mathbf{B}) can be expressed in terms of scalar and vector potentials ϕ and \mathbf{A} as follows [18].

$$\mathbf{B} = \nabla \times \mathbf{A}$$

$$\mathbf{E} = -\nabla \phi - \frac{\partial \mathbf{A}}{\partial t}$$

Thus automatically satisfying Equation(2) and Equation(3). As is well-known [19], in the absence of free charges, the scalar potential can be taken as zero (the so-called Coulomb gauge) and the resulting equation for the vector potential is obtained, by using standard vector identities, as

$$\nabla^2 \mathbf{A} - \mu_0 \epsilon_0 \frac{\partial^2 \mathbf{A}}{\partial t^2} = -\mu_0 \mathbf{J} \quad (5)$$

We first seek a solution for a single-turn coil. This solution is given in Smythe (1989)'s book, but we will show it in somewhat detail for the later parts of the manuscript to be clearer[20]. Locating the origin at the axis of the coil, the coil is located at $r = r_0$ and $\theta = \theta_0$ in spherical coordinates (Fig. 1); and it is a circle of radius

$r_0 \sin \theta_0$ whose center is at a distance $r_0 \cos \theta_0$ from the origin on z-axis.

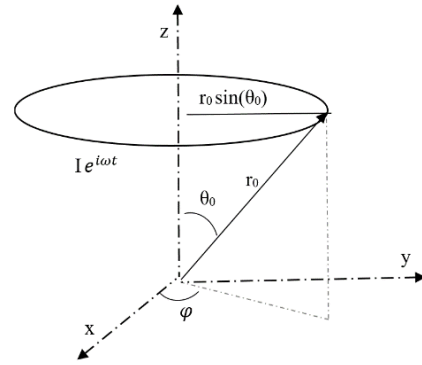


Figure 1. Single turn coil's position in spherical coordinates.

The current density is zero outside of the coil and the coil carries the impressed AC current $I e^{i\omega t}$ with angular frequency ω . Therefore, outside of the coil, we need to solve the homogeneous vector wave equation

$$\nabla^2 \mathbf{A} - \mu_0 \epsilon_0 \frac{\partial^2 \mathbf{A}}{\partial t^2} = 0 \quad (6)$$

Since the system is linear, the solution for the forcing $I e^{i\omega t}$ will also have the time-dependence,

$$\mathbf{A}(\mathbf{r}, t) = \mathbf{A}_0(\mathbf{r}) e^{i\omega t} \mathbf{e}_\phi \quad (7)$$

Using Equation(7) in Equation(6) the only nonzero component of Equation(6) is the phi-component

$$\frac{1}{r} \frac{\partial^2 (rA)}{\partial r^2} + \frac{1}{r^2} \frac{\partial^2 A}{\partial \theta^2} + \frac{\cot \theta}{r^2} \frac{\partial A}{\partial \theta} - \frac{1}{r^2} \frac{1}{\sin^2 \theta} A = 0 \quad (8)$$

Separated and superposed solutions of Equation(8) can be expressed as

$$A = \sum_{n=1}^{\infty} \left(c_n r^n + \frac{d_n}{r^{n+1}} \right) P_n^1(\cos \theta) \quad (9)$$

P_n^1 is the associated Legendre functions (P_n^m with $m = 1$). The coil introduces a simple discontinuity at $r = r_0$.

Expressing the vector potential as

$$A(r, \theta) = \begin{cases} A^{(1)}(r, \theta), & r \leq r_0 \\ A^{(2)}(r, \theta), & r > r_0 \end{cases} \quad (10)$$

and noting the r-terms that blow up in each region, the solution in the two parts can be expressed as

$$A^{(1)} = \sum_{n=1}^{\infty} c_n r^n P_n^1(\cos \theta) \quad (11)$$

$$A^{(2)} = \sum_{n=1}^{\infty} \frac{d_n}{r^{n+1}} P_n^1(\cos \theta) \quad (12)$$

The general "jump conditions" for Maxwell's equations between two media denoted by superscripts are

$$\mathbf{n} \times (\mathbf{E}^{(2)} - \mathbf{E}^{(1)}) = 0 \tag{13}$$

$$\mathbf{n} \times (\mathbf{H}^{(2)} - \mathbf{H}^{(1)}) = \mathbf{J}_s \tag{14}$$

where $\mathbf{H} = \mathbf{B} / \mu_0$ is the magnetic field strength. ρ_s and \mathbf{J}_s are the surface charge and current densities, respectively. \mathbf{n} is the normal vector of the surface separating the two media pointing from region 1 to region 2. There is no surface charge in the present case, and the surface current is restricted to the coil. Equation(11) and Equation(12) are solved together to find the unknown c_n and d_n coefficients. The result is

$$d_n r_0^{-n-1} - c_n r_0^n = 0 \tag{15}$$

$$n d_n r_0^{-n-1} + (n+1) c_n r_0^n + \frac{I \mu_0 (2n+1)}{2n(n+1)} \sin \theta_0 P_n^1(\cos \theta_0) = 0 \tag{16}$$

with the solution

$$c_n = \frac{I \mu_0}{2n(n+1)} r_0^{-n} \sin \theta_0 P_n^1(\cos \theta_0) \tag{17}$$

$$d_n = \frac{I \mu_0}{2n(n+1)} r_0^{n+1} \sin \theta_0 P_n^1(\cos \theta_0) \tag{18}$$

Thus, the vector potential and fields become

$$A^{(1)} = I \mu_0 \sum_{n=1}^{\infty} \frac{1}{2n(n+1)} r_0^{-n} \sin \theta_0 P_n^1(\cos \theta_0) r^n P_n^1(\cos \theta) \tag{19}$$

$$A^{(2)} = I \mu_0 \sum_{n=1}^{\infty} \frac{1}{2n(n+1)} r_0^{n+1} \sin \theta_0 P_n^1(\cos \theta_0) r^{-n-1} P_n^1(\cos \theta) \tag{20}$$

$$\mathbf{E} = -i\omega \mathbf{A} \tag{21}$$

$$\mathbf{B} = \nabla \times (\mathbf{A} \mathbf{e}_\varphi) \tag{22}$$

Note that the electric field is simply proportional to the vector potential and only has an \mathbf{e}_φ component, whereas the magnetic field will be of the form

$$\mathbf{B} = B_r(r, \theta) \mathbf{e}_r + B_\theta(r, \theta) \mathbf{e}_\theta \tag{23}$$

3. MULTI-WINDING SOLUTION

The solution found above is valid for a single-turn coil, or filament, placed at $r = r_0$ and $\theta = \theta_0$. In practice, the coils are not single-turn and normally have a number of turns. To generalize the above solution, consider a multi-winding coil occupying the region $\theta_a < \theta < \theta_b, r_a < r < r_b$. With number of turn N (Fig 2).

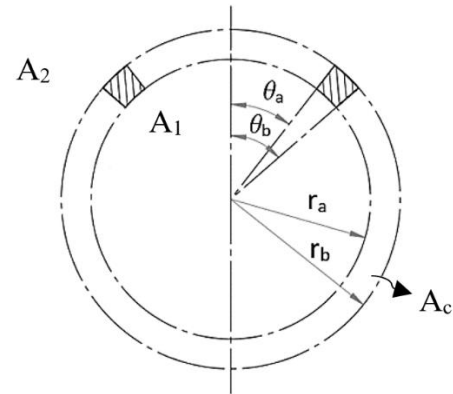


Figure 2 Cross-sectional view of a multi-winding coil.

Cross-sectional area of the coil is

$$S = \frac{1}{2} (r_b^2 - r_a^2) (\theta_b - \theta_a) \tag{24}$$

And the coil is shaped like a spherical strip (not a cylindrical coil). Here r_a, θ_a, r_b and θ_b are the spherical coordinates denoting the location of the coil. The solutions for the regions inside ($r < r_a$) and outside ($r > r_b$) of the coil are obtained by simply integrating the single-turn solution over the cross-section of the coil (i.e., integration is over r_0 and θ_0) multiplied by the number of terms per unit area N/S.

$$\frac{N}{S} \int_{\theta_a}^{\theta_b} \int_{r_a}^{r_b} A(r, \theta, r_0, \theta_0) r_0 dr_0 d\theta_0 \tag{25}$$

Here Equation(19) or Equation(20) is to be substituted for $A^{(0)}$ inside and outside of the N-turn coil. Performing the double integrations, the vector potential for $r < r_a$ is

$$A^{(1)} = \sum_{n=1}^{\infty} C_n r^n P_n^1(\cos \theta) \tag{26}$$

and for $r > r_b$,

$$A^{(2)} = \sum_{n=1}^{\infty} \frac{D_n}{r^{n+1}} P_n^1(\cos \theta) \tag{27}$$

Here,

$$C_n = \frac{N}{S} I \mu_0 \frac{\alpha(r_a, r_b)}{2n(n+1)} \int_{\theta_a}^{\theta_b} \sin \theta_0 P_n^1(\cos \theta_0) d\theta_0 \text{ and}$$

$$D_n = \frac{N}{S} I \mu_0 \frac{r_b^{n+3} - r_a^{n+3}}{2n(n+1)(n+3)} \int_{\theta_a}^{\theta_b} \sin \theta_0 P_n^1(\cos \theta_0) d\theta_0$$

$$\alpha(r_a, r_b) = \left\{ \begin{array}{ll} n=1, & r_b - r_a \\ n=2, & \ln\left(\frac{r_b}{r_a}\right) \\ n>2, & \frac{1}{2-n} (r_b^{2-n} - r_a^{2-n}) \end{array} \right\}$$

In the region $r_b > r > r_a$, the situation is somewhat more involved; since none of them becomes infinite, both $c_n r^n$ and d_n / r^{n+1} terms need to be kept in Equation(9). Denoting the region $r_b > r > r_a$ by a superscript (c), the solution can be expressed as

$$A^c(r, \theta) = \frac{N}{S} \int_{\theta_a}^{\theta_b} \int_{r_a}^r A^{(2)}(r, \theta) r_0 dr_0 d\theta_0 + \frac{N}{S} \int_{\theta_a}^{\theta_b} \int_r^{r_b} A^{(1)}(r, \theta) r_0 dr_0 d\theta_0$$

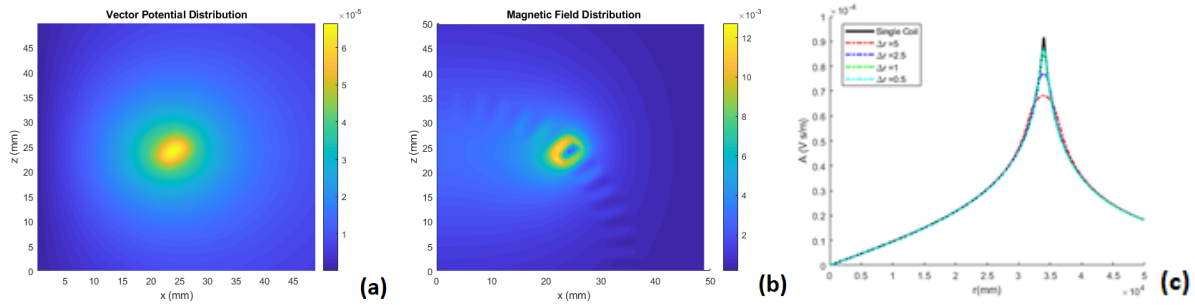


Figure 3 Distribution of **A** (a). Distribution of **B** (b). **A** for different Δr (c).

$$(28)$$

And the result is

$$A^c = \left[F_n(r)r^n + \frac{G_n(r)}{r^{n+1}} \right] P_n^1(\cos \theta_0), \quad r_b > r > r_a \quad (29)$$

Here

$$F_n(r) = \frac{N}{S} I \mu_0 \frac{\beta(r)}{2n(n+1)} \int_{\theta_a}^{\theta_b} \sin \theta_0 P_n^1(\cos \theta_0) d\theta_0 \quad \text{and}$$

$$\beta(r) = \begin{cases} n=1, & r_b - r \\ n=2, & \ln\left(\frac{r_b}{r}\right) \\ n>2, & \frac{1}{2-n}(r_b^{2-n} - r^{2-n}) \end{cases}$$

$$G_n(r) = \frac{N}{S} I \mu_0 \frac{r^{n+3} - r_a^{n+3}}{2n(n+1)(n+3)} \int_{\theta_a}^{\theta_b} \sin \theta_0 P_n^1(\cos \theta_0) d\theta_0$$

The electric fields (**E**) and magnetic fields (**B**) can be computed from Equation(21) and Equation(22).

4. ANALYTICAL AND FEM RESULTS

In this section, we present computations based on the formulas obtained in section 3; also, numerical simulations based on the finite element capabilities of the commercial ANSYS software will be presented for comparison. To form a better understanding, we define

the coil by its center $r_c = \frac{r_a + r_b}{2}$, $\theta_c = \frac{\theta_a + \theta_b}{2}$ and its

range ($\Delta r = r_b - r_a$, $\Delta \theta = \theta_b - \theta_a$). Figure 3 shows the vector potential as a function of r with $r_a < r < r_b$ for coils centered at $\theta_m = 45^\circ$ with $\Delta \theta = 10^\circ$ and for various Δr ($I=1A$, $N=100$ turns and $\mu_0 = 4\pi \cdot 10^{-7} H/m$). Note that, as Δr gets smaller, vector potential increases around the region where the coil is located. It becomes singular (infinite) for a single-turn coil (placed at the center of the multi-turn coil), as it should. In the multi-winding coil, the singularity is eliminated (Figure 3c). The contours of vector potential and magnetic field are given in Figure 3, using the same coil as before. The position of the coil can be clearly seen in both figures.

The same configurations were also solved by using the commercial ANSYS software, which uses the finite element method. The results are shown in Figure 4. The results are very close away from the coil, but the analytical results are sharper at the coil corners. Here $\Delta \theta = 10^\circ$, $r_0 = 34mm$, $\Delta r = 5mm$, $\theta_0 = 45^\circ$

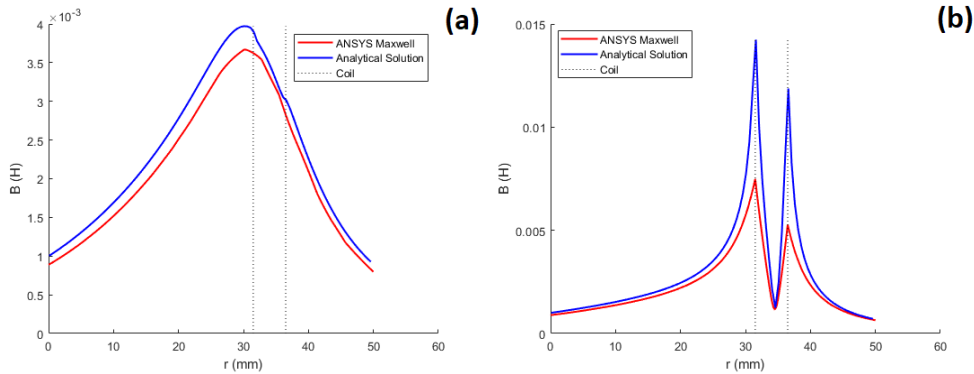


Figure 4 Distribution of **B** with r in $\theta = 30^\circ$ (a). Distribution of **B** with r in $\theta = 45^\circ$ (b).

5. CALCULATION OF INDUCTANCE COEFFICIENTS

Self-inductance (L) is defined as the induction of a voltage in a current-carrying wire when the current in the wire itself is changing. Voltage created on the N-turn coil is

$$V = -i\omega \frac{N}{S} \iint_{dS} \left\{ \iint_{(r_0, \theta_0)} \mathbf{A} \cdot d\mathbf{r} \right\} dS \tag{30}$$

The innermost curvilinear integral is the voltage created on a single turn coil at (r_0, θ_0) ; here, \mathbf{E} is $\mathbf{E}(r_0, \theta_0)$.

This voltage is integrated over the cross-section and multiplied by turns per area. Over the cross-section, A is $A^{(c)}$ given by Equation(29). With the definition

$$Q_n(\theta_a, \theta_b) = \int_{\theta_a}^{\theta_b} \sin \theta_0 P_n^1(\cos \theta_0) d\theta_0$$

Impedance is

$$L = \pi\mu_0 \frac{N^2}{S^2} \sum_{n=1}^{\infty} Q_n^2 \int_{r_0=r_a}^{r_0=r_b} \frac{1}{n(n+1)} \left(\frac{r_0^{n+3} - r_a^{n+3}}{(n+3)} r_0^{-n+1} + \beta(r_0) r_0^{n+2} \right) dr_0 \tag{31}$$

Another practically important quantity is the mutual inductance between two coils M_{12}^c . To calculate it, let's consider two concentric coils in spherical coordinates as shown in Figure 5(a). Here, γ is the angle between the coils' axes, α and β are the angular coordinate of the coils with respect to their set of axes, a and b are the r coordinates where the coils are located. The representation of the coils as multi-windings is given in Figure 5(b). The coil with the N_1 number of windings and radius a is located in the γ position in spherical coordinates. The vector potential of $A^{(b)}(b, \theta')$ which the coil creates is given by Equation(27).

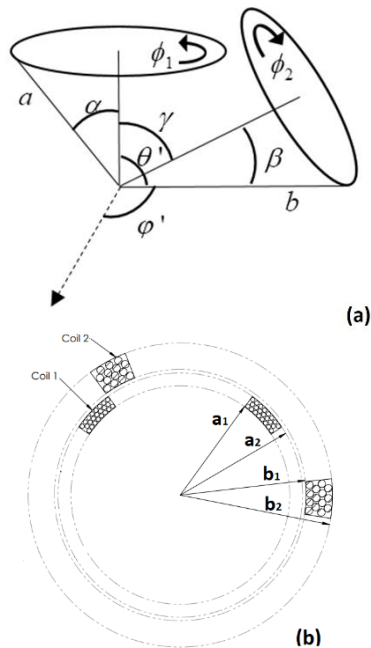


Figure 5. Concentric single-winding coils (a)[20]. Concentric multi-winding coils (b).

Where

$$M_{12} = \pi\mu_0 \frac{N_1 N_2}{S_1 S_2} \sum_{n=1}^{\infty} \frac{W_n(\alpha_1, \alpha_2)}{n(n+1)} \left(\frac{b_2^{n+3} - b_1^{n+3}}{n+3} \right) P_n(\cos \gamma) Q_n(\alpha_1, \alpha_2) Q_n(\beta_1, \beta_2) \tag{32}$$

$$W_n(a_1, a_2) = \begin{cases} n=1, & a_2 - a_1 \\ n=2, & \ln\left(\frac{a_2}{a_1}\right) \\ n>2, & \frac{1}{2-n} (a_2^{2-n} - a_1^{2-n}) \end{cases}$$

Equation(31) and Equation(32) are used to calculate the self-inductance and mutual-inductance of a multi-winding coil.

6. EXPERIMENTAL RESULTS

Parameters of the experimental set are as defined in Figure 5 and Figure 6. Numerical values of the parameters are given in Table 2. The bodies were manufactured by 3D printing using a plastic material. 3D printers have been used in the manufacture of many experimental setups in the literature[21-22]. The explanations of the numbers in Figure 6 are shown in Table 1. Coil 1 is wrapped on the body1 as 180 turns of wire with a diameter of Ø0.75 mm. Coil 2 is wrapped on the body2 as 150 turns of wire with a diameter of Ø0.5 mm.

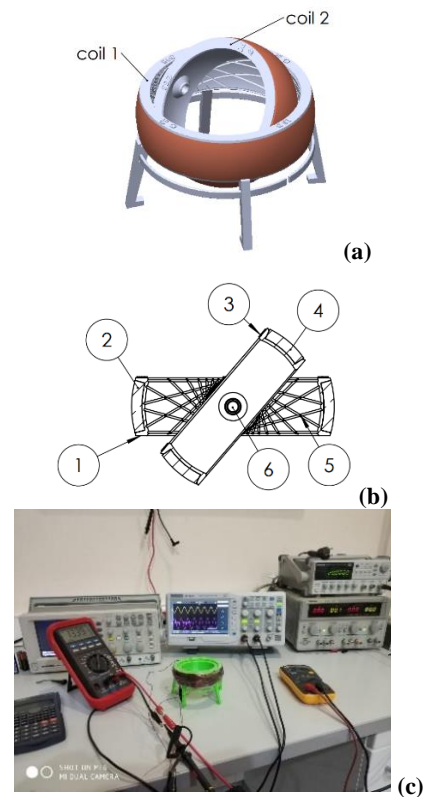


Figure 6. 3D view of test set (a), Coil layouts (b). Experiment set (c).

Table 1. Test parts description.

Part number	Description
1	Body part on which the fixed coil is wound
2	Fixed coil windings
3	Body part on which the moving coil is wound
4	Moving coil windings
5	Angle lines of 15° degrees.
6	Rotation center

Table 2. Manufactured coil parameters.

Parameters	Coil 1	Coil 2
r_1	$a_1=44$ mm	$b_1=36.5$ mm
r_2	$a_2=49$ mm	$b_2=41.5$ mm
θ_1	$\alpha_1=75^\circ$	$\beta_1=75^\circ$
θ_2	$\alpha_2=105^\circ$	$\beta_2=105^\circ$
γ	0	0 - 180
N	180	150
D_c	0.75 mm	0.5 mm
R1, R2	2.6 ohm	3.35 ohm
R3	10.4 ohm	

The self-inductance coefficient (L) was directly measured with the LCR meter. However, it is not possible to directly measure the mutual inductance coefficient (M_{ij}). In order to evaluate the mutual inductance coefficient, the fixed coil was connected to a constant AC power supply, 50 Hz, 12 V (mains voltage reduced by a transformer). A resistor (1 ohm) is used for limiting the current on Coil 1. Voltage V2 on the moving coil was measured while varying the angle γ between the coils in 15° increments. It was seen that the error values obtained in the analytical calculation and FEM results are very close to each other (Fig 7), and the results obtained in the experimental study differ 10% from both of them.

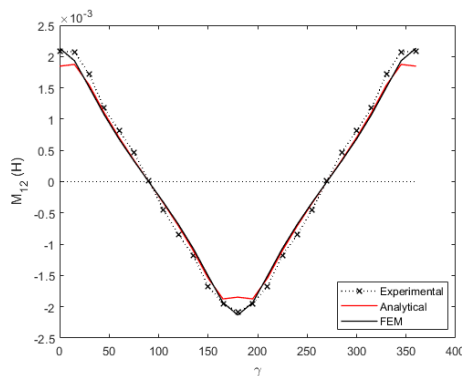


Figure 7. Comparison of M_{12} Experimental results, analytical results and FEM results at different values of γ

7. CONCLUSION AND DISCUSSION

In this study, first, a magnetic coil with an air core was defined in spherical coordinates, and magnetic field \mathbf{B} and electric field \mathbf{E} expressions were calculated analytically. The formulas derived for the single coil are compatible with the formulas in the literature [20]. In the multi- turn case, as the coil winding width Δr shrinks, the results get closer to single-coil results. When the magnetic field \mathbf{B} expression was examined on the x-z plane, errors are seen due to the singularity that occurs in the area where the coil was located. Elimination of the singularity may be an interesting research topic.

As a result, it was seen that the \mathbf{B} distribution obtained with the multi- turn coil case with the proposed method is compatible with the finite element program (FEM) results. The variation of mutual inductance (M_{12}) between the two coils with the angle γ were calculated analytically, and confirmed experimentally. The deviations between the results are thought to be due to the fact that the windings used in the application are made manually, and also due to the singularity resulting from the Legendre polynomials used in the calculation of the analytical results. The analytical solution of Maxwell's equations in spherical coordinate system has been explained in detail and it has been shown that the results obtained in the multi-turn coil approach are close to those obtained with FEM and experimental results. Each result seems to be close to experimental data. Analytical results are compatible with FEM results. FEM programs are known to be costly and require long calculation times. Therefore, it can be concluded that analytical computations can be used as a fast and free design tool (instead of costly and time-consuming FEM computations) during scientific studies and preliminary design steps.

DECLARATION OF ETHICAL STANDARDS

The author(s) of this article declare that the materials and methods used in this study do not require ethical committee permission and/or legal-special permission.

AUTHORS' CONTRIBUTIONS

Hüseyin YILDIZ: Performed the experiments and the analytical results.

Erol UZAL: Performed the analytical the results.

Hüseyin ÇALIK: Performed the experiments and analyse the results.

CONFLICT OF INTEREST

There is no conflict of interest in this study.

REFERENCES

- [1] Ravaud, R., Lemarquand, G., Lemarquand, V., Babic, S., & Akyel, C., "Mutual inductance and force exerted between thick coils", *Progress In Electromagnetics Research*, 102: 367-380, (2010).

- [2] Conway, J. T., "Mutual inductance for an explicitly finite number of turns", *Progress In Electromagnetics Research B*, 28: [273-287](#), (2011)
- [3] Babic S. I. and Akyel C., "New analytic-numerical solutions for the mutual inductance of two coaxial circular coils with rectangular cross section in air", *IEEE Transactions on Magnetics*, 42(6): [1661-1669](#), (2006)
- [4] Conway, J. T., "Exact solutions for the mutual inductance of circular coils and elliptic coils", *IEEE transactions on magnetics*, 48(1): [81-94](#), (2012)
- [5] Lipinski, W., Rolicz, P., & Sikora, R., "Application of integral transforms to the analysis of the magnetic field of a spherical coil", *IEEE Transactions on Magnetics*, 11(5): [1552-1554](#), (1975).
- [6] Semenov, V. G., "Synthesis of spherical methods of determining magnetic field source parameters of internal and external origin", *Measurement Techniques*, 33(12): [1236-1240](#), (1990).
- [7] Eaton, H., "Electric field induced in a spherical volume conductor from arbitrary coils: application to magnetic stimulation and MEG", *Medical and Biological Engineering and Computing*, 30(4): [433-440](#), (1992).
- [8] Matute, E. A., "On the vector solutions of Maxwell equations in spherical coordinate systems". *arXiv preprint physics*, [0512261](#), (2005).
- [9] Liu, C. Y., Andalib, T., Ostapchuk, D. C. M., & Bidinosti, C. P., "Analytic models of magnetically enclosed spherical and solenoidal coils", *Nuclear Instruments and Methods in Physics Research Section A: Accelerators, Spectrometers, Detectors and Associated Equipment*, 949: [162837](#), (2020).
- [10] Lee, K. M., Son, H., & Joni, J., "Concept development and design of a spherical wheel motor (SWM)", *In Proceedings of the 2005 IEEE International Conference on Robotics and Automation*: [3652-3657](#), (2005).
- [11] Dehez, B., Galary, G., Grenier, D., & Raucant, B., "Development of a spherical induction motor with two degrees of freedom", *IEEE Transactions on Magnetics*, 42(8): [2077-2089](#), (2006)
- [12] Fernandes, J. F., & Branco, P. C., "The shell-like spherical induction motor for low-speed traction: electromagnetic design, analysis, and experimental tests". *IEEE transactions on industrial electronics*, 63(7): [4325-4335](#), (2016).
- [13] Zhang, C., Yuan, L., Zhang, J., Chen, J., Chen, C. Y., Chen, S., & Yang, G., "Analytical models of electromagnetic field and torques in a novel reaction sphere actuator", *In 2018 IEEE International Conference on Applied System Invention (ICASI)*, [271-274](#), (2018a).
- [14] Zhang, J., Yuan, L., Liao, Y., Zhang, C., Chen, C. Y., Chen, S., & Yang, G., "Torque optimization of a novel reaction sphere actuator based on support vector machines". *In 2018 IEEE International Conference on Applied System Invention (ICASI)*, [263-266](#), (2018b).
- [15] Zhou, H., Fang, Y., & Ma, J. Structural Design and FEA of a New Type of Multi-DOF Spherical Induction Motor without Output Shaft. *In 2019 22nd International Conference on Electrical Machines and Systems (ICEMS)*, (1-7). IEEE., (2019a, August).
- [16] Akkaya Oy, S., Arslan, S. & Gürdal, O., "Finite Element Analysis of the Inductance and Magnetic Field in the Permanent Magnet Spherical Motor", *Politeknik Dergisi*, 23 (4), [1387-1394](#) (2020)
- [17] Kuang, S., & Yan, G., "Modelling on mutual inductance of wireless power transfer for capsule endoscopy", *Biomedical Microdevices*, 22(3), [1-11](#), (2020)
- [18] Jackson, J. D., "*Classical electrodynamics*", John Wiley & Sons, ISBN-13: 978-0471309321, Inc, New York, (1962).
- [19] Griffiths, D. J., "*Introduction to Electrodynamics*", Prentice Hall, ISBN 0-13-805326-X, New Jersey, (1998).
- [20] Smythe, W. R., "*Static and dynamic electricity*", Taylor & Francis Publisher, ISBN-13: 978-0891169161, New York, (1989).
- [21] Hacıoğlu, A., Yılmaz, H. & Ustundag, C. B., "3D Printing for Tissue Engineering Applications", *Politeknik Dergisi*, 21 (1), [221-227](#), (2018).
- [22] Seçkin, M., Seçkin, A. Ç. & Yaman Turan, N., "Investigation of Discharge Characteristics of Hinges Produced with 3D Printing for Prosthetic Fingers". *Politeknik Dergisi*, 24 (2), [575-583](#), (2021)